CORE-HALO LIMITS AND BEAM HALO FORMATION DYNAMICS

M. Valette†, CERN-TE, Geneva, Switzerland
P.A.P. Nghiem, N. Pichoff, CEA/DRF/Irfu, Saclay, France

Abstract

In high intensity linear accelerators, space charge related instabilities and effects are the cause of emittance increase and beam losses. The mechanism of halo formation due to a mismatched beam causing parametric resonances and energy transfer between phase-spaces is one of them. The previously defined one dimensional core-halo limit [1-3] was extended to two-dimensional distributions [4]. This halo characterization method is applied to a classical case of transport for halo formation studies: the transport of a mismatched beam. Our method provides a core-halo limit that matches the expected halo formation mechanism with a very good precision.

INTRODUCTION

The previously defined two-dimensional core-halo limit [4] is determined solely based on distribution of particles in the two-dimensional phase-space. It is interesting to know if this limit reflects the halo formation dynamics. For this we consider the well-known study of transporting a mismatched beam to establish that the halo so defined corresponds to the halo created by the effect of space-charge.

CONSIDERED TRANSPORT

We consider the transport of a 100mA, 5MeV proton beam so as to be in conditions close to currently designed high intensity linacs and studies on instabilities caused by mismatch in the presence of space-charge [5-7].

The beam is transported through a continuous focusing channel of total length 300m. To have reliable statistics, a distribution of 1 million macro-particles uniformly distributed in a 6D ellipsoid is used as input. The beam therefore has initially no halo in 6D phase-space.

We select for this transfer line the following three phase advances (non-depressed or without space-charge) in order to have the least possible coupling between the 3 phase-spaces: $\mu_{0x} = 80$, $\mu_{0y} = 65$ and $\mu_{0z} = 30$ degrees.m^{-1}.

Provided we adopt for the input beam the RMS emittances: $\varepsilon_x = 1$, $\varepsilon_y = 2$ and $\varepsilon_z = 10$ µm, the 100 mA matched beam for this structure must have $\beta_x = 0.81$, $\beta_y = 1$ and $\beta_z = 2.14$ m, with all α-parameters being zero. This beam will experience "weak" space-charge effects and have a tune depression ratio of 0.9 in all three phase-spaces with depressed phase-advances: $\mu_x = 71$, $\mu_y = 58$ and $\mu_z = 27$ degrees.m^{-1}.

While keeping the same focusing structure and all the same Twiss parameters, we fabricate a mismatched beam by only lowering the vertical size by lowering its emittance to $\varepsilon_y = 0.7$ µm. The three phase advances become $\mu_x = 69$, $\mu_y = 52$ and $\mu_z = 26$ degrees.m^{-1}. The tune depression is thus much stronger for the (y,y') plane and stronger space-charge effects are expected in this plane only.

SIMULATION RESULTS

The transport simulations were done with the TraceWin code [8]. For the aforementioned mismatched beam, the input and output distributions of particles are respectively shown in Fig. 1 and Fig. 2. The vertical distribution of particles along beam transport are presented in Fig. 4 for both the matched and the mismatched beam.

In the matched case, the final emittances in all three phase-spaces are identical to the initial ones, within numerical errors. In the mismatched case, final emittances are: $\varepsilon_x = 1$, $\varepsilon_y = 0.8$ and $\varepsilon_z = 9.9$ µm. One can note the vertical emittance increase. But there is also an emittance transfer to the longitudinal plane due to the 1:2 phase-advance parametric resonance being excited by mismatched-induced beta beating [9]. Nevertheless, this effect remains limited thanks to the low space charge in this plane.

In case of matched beam, the particle distribution remains unchanged in shape as well as in total size along transport. On the contrary, when the beam is mismatched, a gradual increase in size and distribution appearance in the (y,y') plane takes place from longitudinal coordinate 40m, which stabilizes around 150m. The distribution does not change in the horizontal plane while in the longitudinal plane filamentation can be observed in the output distribution involving a small number of particles.

Numerous studies on halo formation dynamics (some of which are mentioned above) predict that a mismatched beam will undergo emittance increase and halo development. The latter being composed of particles which have undergone nonlinear transport causing them to have more external positions [10].

The core-halo limit determined by methods detailed in a previous publication [4] was reported in Fig. 2 for each of the phase-spaces. We can first say that this limit is qualitatively in agreement with this vision of halo formation. Indeed, this limit clearly indicates that there is practically no halo for the input beam, nor for the final one in case of matched transport, and on the contrary confirms the presence of halo in case of mismatch. Quantitatively, this method also gives precisely the number of macro-particles in the halos of different phase spaces (for a total sample of one million particles):

- input beam: 13 in (x,x'), 29 in (y,y'), 44 in (z,z').
- output beam: 17 in (x,x'), 4328 in (y,y'), 1489 in (z,z').

I.e. the PHP* and PHS** parameters: (0,0) in (x,x'), (0.3,14) in (y,y')and (0.01,0.9) in (z,z').

† matthieu.valette@cern.ch

* Percentage of Halo Particles
** Percentage of Halo Surface

ISBN 978-3-95450-147-2

This confirms that, within numerical errors, the halo-less 6D input distribution has no halo in all phase-spaces with our definition. Moreover, a significant halo has developed in the two-dimensional phase-spaces where the beam is mismatched and those coupled by parametric resonances.

SINGLE PARTICLE AND HALO FORMATION DYNAMICS

We will now study the agreement between the core-halo limit and halo-formation dynamics in more details. For this we propose to consider the emittance of individual particles. We recall that in the case of linear transport in a continuous focusing channel, without space-charge, the trajectory of each particle describes a perfect ellipse in phase-space. The surface of this ellipse gives the characteristic emittance, or action, of the particle, which is a transport invariant. In the case of matched transport with space-charge, space-charge forces disturb these paths and the periodical positions of particles in phase-space form a cloud of points around an ellipse. We can determine a fitted ellipse from these positions [11] and calculate its area to determine the single particle emittances, which can change during nonlinear transport.

Let us examine single particle emittances in the (y, y') phase-space along the considered transport over the first 20 and the last 20 meters of the structure, respectively noted ε_{init} and ε_{end}. Fig. 3 shows the normalised histograms of the $\varepsilon_{end}/\varepsilon_{init}$ ratios for all transported particles in three cases:

1. Without space-charge, for which the ratio is 1 for each particle, the histogram can be summed up by a delta function in 1.
2. Matched beam with space-charge, for which the histogram is a symmetrical distribution around 1 with a certain width.
3. Mismatched beam with space-charge, for which the distribution is wider, with a small surplus of particles with a ratio greater than 1.

These results can be understood by considering the dynamics of particles. In the first case, only undergoing linear external forces, their movement are those of pure harmonic oscillators, neither gaining nor losing transverse energy.

In the second case, nonlinear space charge forces bring up small perturbations on the movement of particles. With good enough statistics, for most macro-particles, effects felt during the oscillations compensate each other and their average effect is null. As a result, the histogram is symmetric around 1.

In the third case, the effect of space charge is more important in the y direction. Because of mismatch, the beam envelope will be oscillating and some particles, in phase with this beating, can win or lose a lot of transverse energy, which explains the greater width of the histogram. In this context, some particles may have sufficiently disturbed trajectories to gain enough energy and find themselves in an outer part of the distribution, the halo. Where they will remain because the period of their betatron oscillations will be sufficiently different from those of the rest of beam, as they will feel the nonlinear part of the space-charge field.

IDENTIFICATION OF HALO PARTICLES

According to this halo-formation dynamics, core particles can have a $\varepsilon_{end}/\varepsilon_{init}$ ratio greater or less than 1, while the particles of the halo must necessarily have larger than 1 ratios. In fact, as there was initially no halo in the transported distribution, the particles which are located in the halo at the end must necessarily have undergone an emittance increase.

Let us now consider the $\varepsilon_{end}/\varepsilon_{init}$ ratio histogram in the case of the mismatched beam, but sorting particles that are in the core or the halo using the previously determined core-halo limit. The histogram of the core should have a distribution centred on 1 while the one of the halo should be located exclusively above 1.

Such histograms are shown in Fig. 5. It is apparent that the halo particles mostly have greater than 1 ratio, but there are however a small number with ratios around 1.

It should be noted that due to the much denser core, even a very small error in the position of the core-halo limit, whether due to numerical noise or intrinsic to the method, will result in a non-negligible number of core particles being considered as part of the halo. In our case, by simply increasing the coordinates of all the points of the contour by 4% one can see that the halo particles have exclusively ratios above 1 as expected and shown in Fig. 6.

CONCLUSION

We thus conclude that the core-halo limit determined in two-dimensional phase-spaces by the maximum of the second-derivative criterion:

- corresponds to what is expected by visual examination.
- is qualitatively and quantitatively consistent with the halo-formation dynamics with a few percent error.

REFERENCES

[1] Nghiem *et al.*, *Appl. Phys. Lett.*, vol. 104, p. 074109, 2014.

[2] Nghiem *et al.*, *Physics of Plasma*, vol. 22, P. 083115, 2015.

[3] Nghiem *et al.*, in *Proc. of IPAC'15*, Richmond, Virginia, USA, 2015.

[4] Valette *et al.*, in *Proc. of IPAC'15*, Richmond, Virginia, USA, 2015.

[5] M. Lund *et al.*, *Nucl. Instrum. Meth. Phys. Res.* A, 561, 2006.

[6] J. Barnard *et al.*, in *Proc. of PAC97*, Vancouver, British Columbia, Canada, 1997.

[7] J. Quiang *et al.*, In *Proc. of PAC99*, New York City, New York, USA, 1999.

[8] Duperrier, Pichoff & Uriot, in *Proc. of ICCS2002*, Amsterdam, Netherlands, 2002.

[9] J. Quiang *et al.*, in *Proc. of PAC2001*, Chicago, Illinois, USA, 2001.

[10] R.P. Nunes *et al.*, *Physics of plasma*, 16, 2009.

[11] M. Valette, PhD thesis, Paris Saclay University, 2015

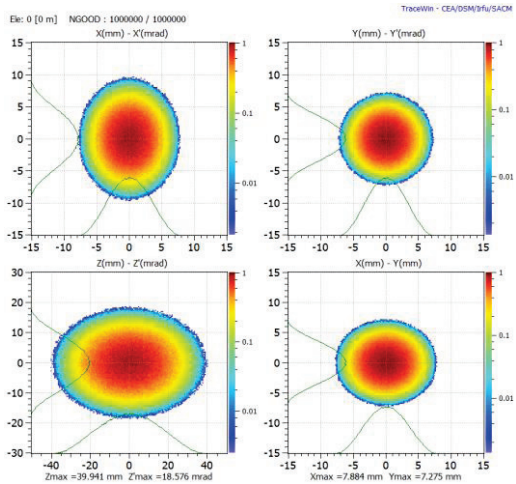

Figure 1: Distribution of the input beam in various phase-spaces in the mismatched case.

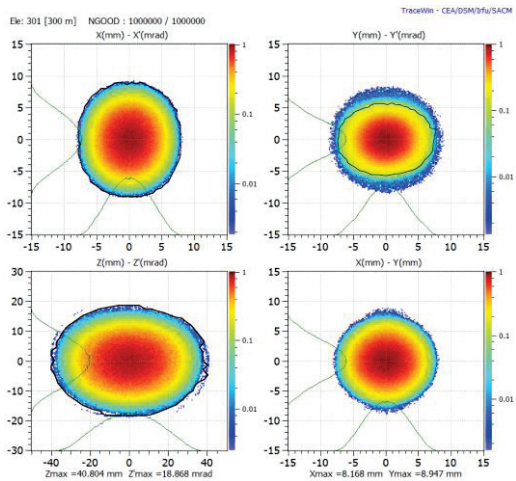

Figure 2: Distribution of the output beam in various phase-spaces in the mismatched case. The black line shows the computed core-halo limit.

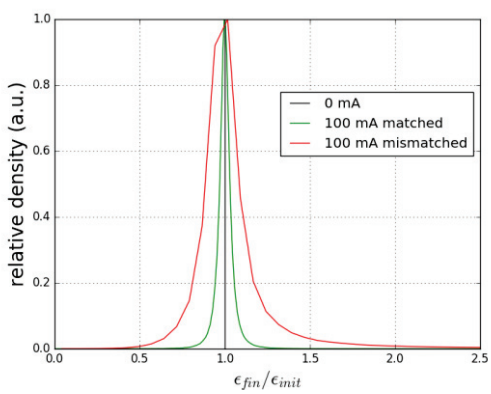

Figure 3: Histograms of single particle emittance variation ratio for transport without space-charge and with space-charge in the matched and mismatched case.

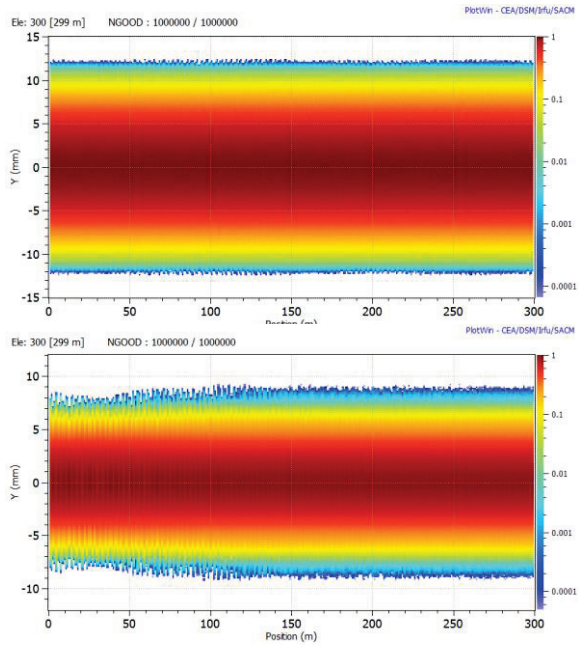

Figure 4: Beam distribution in the vertical plane along the transport of the matched (top) and mismatched (bottom) beams.

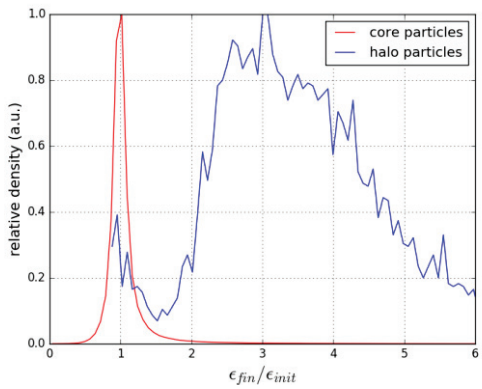

Figure 5: Histograms of single particle emittance variation ratio of core and halo particles in the mismatched case.

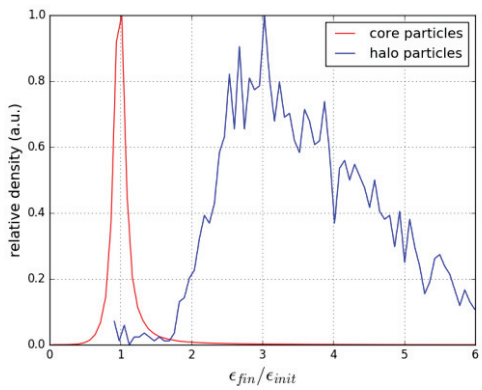

Figure 6: Histograms of single particle emittance variation ratio of core and halo particles in the mismatched case, with a 4% dilated contour.

ISBN 978-3-95450-147-2